Flame Spread Mechanism of a Blended Fuel Droplet Array at Supercritical Pressure

Takeshi Iwahashi
Toyota Motor Corporation
Toyota, Aichi 471-8572, Japan

Hideaki Kobayashi and Takashi Niioka
Institute of Fluid Science
Tohoku University
Sendai, Miyagi 980-8577, Japan

ABSTRACT

Flame spread experiments of a fuel droplet array were performed using a microgravity environment. N-decane, 1-octadecene, and the blends (50% : 50% vol.) of these fuels were used and the experiments were conducted at pressures up to 5.0 MPa, which are over the critical pressure of these fuels. Observations of the flame spread phenomenon were conducted for OH radical emission images recorded using a high-speed video camera. The flame spread rates were calculated based on the time history of the spreading forehead of the OH emission images.

The flame spread rate of the n-decane droplet-array decreased with pressure and had its minimum at a pressure around half of the critical pressure and then increased again with pressure. It had its maximum at a pressure over the critical pressure and then decreased gradually. The pressure dependence of flame spread rate of 1-octadecene were similar to those of n-decan, but the magnitude of the spread rate was much smaller than that of n-decane. The variation of the flame spread for the blended fuel was similar to that of n-decane in the pressure range from atmospheric pressure to near the critical pressure of the blended fuel. When the pressure increased further, it approached to that of 1-octadecene. Numerically estimated gas-liquid equilibrium states proved that almost all the fuel gas which evaporated from the droplet at ordinary pressure consisted of n-decane whereas near and over the critical pressure, the composition of the fuel gas was almost the same as that of the liquid phase, so that the effects of 1-octadecene on the flame spread rate was significant.

Keywords : droplet array, critical pressure, flame spread

INTRODUCTION

Investigation of spray combustion in a high-pressure environment is important for improving control of practical high-loaded combustors and for developing sustainable combustion technology. The mechanism of spray combustion over the critical pressure is particularly interesting from a scientific point of view because the thermal and transport properties of liquid fuel drastically change in this pressure range.

Research using a model of flame spread of a fuel droplet array has been performed to simulate the fundamental flame propagation mechanism of fuel spray [1]. However, because the size of a flame is much larger than that of a single droplet, strong buoyancy is generated, especially at high pressure. Therefore, a microgravity environment is useful for conducting such experiments. Yoshida et al. performed flame spread experiments on droplet arrays of n-heptane, ethanol, and n-undecane using a drop facility and showed that the flame spread rate decreased monotonously with pressure [2]. The maximum pressure of their experiment was 0.5 MPa, which was lower than the critical pressure of the fuels. The present authors performed flame spread experiments on n-decane and n-hexadecane droplet arrays in normal gravity [3] and on n-decane in microgravity at pressures up to 5.0 MPa [4].

In the present study, we extended the flame spread experiments to those using 1-octadecene and blended fuel in microgravity, and herein discuss the effects of pressure and vaporization characteristics of the blended fuel on the flame spread phenomena.

EXPERIMENTAL APPARATUS

Microgravity experiments were performed using the drop-shaft facility of the Microgravity Laboratory of Japan (MGLAB) located in the city of Toki. The free-fall length, the test duration and the quality of microgravity of the facility are 100 m, 4.5 s, and 10^{-5}g, respectively.

Figure 1 shows the experimental setup installed in a payload rack of MGLAB' s drop capsule. The apparatus consists of a high-pressure chamber, an image intensifier, a high-speed video system, a CCD video camera, optical mirrors, a note-book computer, and so on. The high-pressure chamber is cylindrical with an inner diameter of 260 mm and an inner length of 410 mm. The chamber has 4 observation windows in total with inner diameters of 50 mm. One of the windows is made of quartz glass through which OH emission images can be observed, and the others are made of BK-7. A gig to support the silica fibers, an igniter, a microsyringe, and a 3-axis stage manipulator were installed in the chamber. The temperature in the high-pressure chamber was close to room temperature.

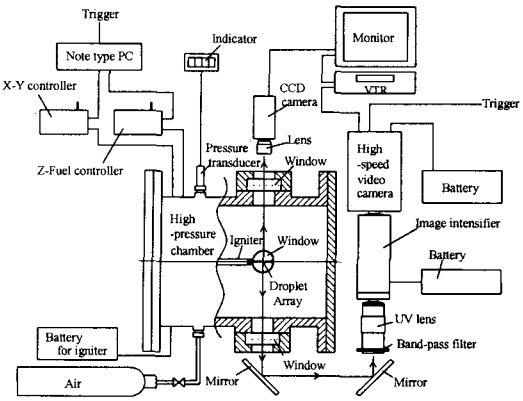

Fig. 1 Schematics of experimental apparatus.

A droplet array was arranged using the fiber

suspension method. Each droplet was suspended at the end of a fine silica fiber 135±5 μm in diameter, the spherical end being 300 ±25 μm in diameter. A maximum of 14 silica fibers was arranged with all spherical ends of the fibers on a line horizontally with equal spacing.

In order to produce a droplet array with equal diameter, a precision droplet generator consisting of a microsyringe driven by a stepping motor and 3-axis automatic stage manipulator was developed. Because the shape of each suspended droplet was ellipsoidal, the equivalent droplet diameter was calculated using the following formula:

$$D=(D_1D_2^2)^{1/3}, \quad (1)$$

where D_1 and D_2 are the short and long diameters, respectively.

The droplet at the end of the array was ignited using a Kanthal wire coil. An electric current of 8 A was supplied for 0.7 s to ignite the droplet at the end of the array. In this experiment, OH emission images were recorded to measure the flame spread rate. A bandpass filter with a center wavelength of 310 nm, which is the peak of the (0,0) band of the OH radical, a UV lens, an image intensifier, and a high-speed video system were used to record the OH emission images during the flame spread at 30 to 600 frames/s. An ordinary CCD video camera was also used to observe the flame.

The fuels used in this experiment were n-decane ($C_{10}H_{22}$, T_b=447 K, T_c=618 K, and P_c=2.11 MPa, where T_b, T_c, P_c are standard boiling temperature, critical temperature, and critical pressure, respectively), 1-octadecene ($C_{18}H_{36}$, T_b=558 K, T_c=739 K, and P_c=1.13 MPa), and blends of these fuels. Equivalent droplet diameter, D, and droplet spacing, S, were 1.0 mm and 2.0 mm, respectively. In the case of the blended fuel, the volume fractions of n-decane and 1-octadecene are 50% and 50%, respectively, corresponding to molar fractions of 62% and 38%. Estimated properties of the blended fuel were T_b=467 K, T_c=685 K, and P_c=2.56 MPa.

Before the drop-capsule release, the droplet array was produced automatically. Just after production of the droplet array, the capsule was released and then ignited. Recorded high-speed OH images of the spreading flame were analyzed after the capsule was recovered. The time history of the locus of the OH emission forehead of spreading flame was plotted and the flame spread rate was calculated from the gradient of the plot.

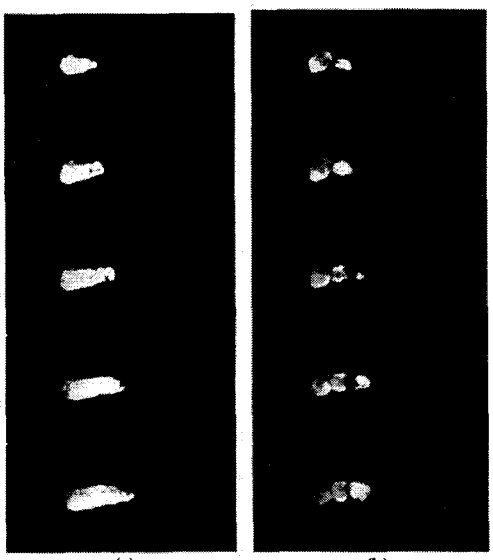

(a) (b)

Fig. 2 OH emission images(S=2.0mm) : (a)1-octadecene, 2.0 MPa; (b) blended fuel, 3.0 MPa

RESULTS AND DISCUSSION

OH Emission Images of Spreading Flame

Figure 2 shows the OH emission images of 1-octadecene and blended fuel. In the case of 1-octadecene (Fig. 2a), a relatively smooth

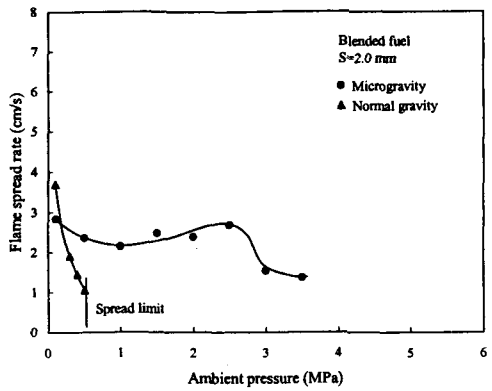

Fig. 3 Variations of flame spread rate of the blended-fuel droplet-array in microgravity and normal gravity.

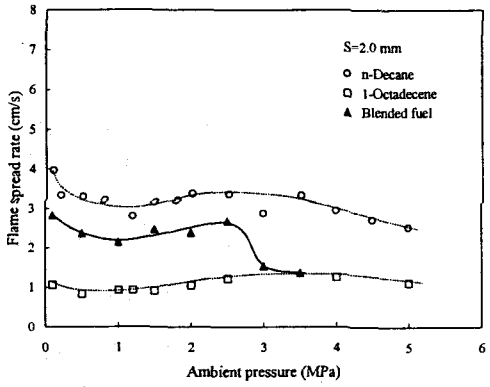

Fig. 4 Variations of flame spread rate of n-decane, 1-octadecene, and blended-fuel droplet-arrays in

flame spread was observed. On the other hand, in the case of blended fuel, zigzag and intermittent flame spread was often seen, similar to the case of the n-decane droplet array near and over the critical pressure [4]. In the case of the n-decane droplet array, it was previously found [4] that fuel vapor jets due to Marangoni convection are issued from the unburned droplet in the pressure range near the critical pressure, causing zigzag-like the flame spread. Therefore, a fuel-vapor jet was also expected to occur in the case of the blended fuel droplet array.

Flame Spread Rates of Single and Blended Fuel Droplet Arrays

Figure 3 shows variations of the flame spread rate with pressure for the blended fuel in microgravity and normal gravity. In normal gravity, the flame spread rate monotonously decreased with pressure and reached the flame spread limit at a certain pressure. This is due to the strong buoyancy effects at high pressure. On the other hand, in microgravity, flame spread occurred at pressures up to 3.5 MPa, which was the maximum pressure of the experiments for the blended fuel.

Figure 4 shows comparisons of the flame spread rate between n-decane, 1-octadecene, and the blended fuel in microgravity. The flame spread rate of the 1-octadecene droplet array is smaller than that of n-decane, but its dependence on pressure appears to be similar to that of n-decane. For n-decane and 1-octadecene droplet arrays, it can be seen that the flame spread rates decrease with pressure and reach the minimum and then increase again with pressure. It has been explained that this variation is basically caused by enhancement of fuel transportation due to the generation of a fuel vapor jet from the unburned

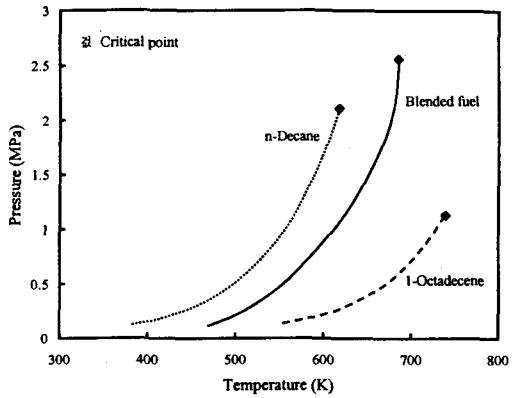

Fig. 5 Vapor pressure curves for n-decane, i-octadecene, and the blended fuel.

droplet mentioned above.

When the mechanism of the small flame spread rate of the 1-octadecene droplet array compared with that of n-decane is investigated, we should consider the difference of the molar latent heat of vaporization between n-decane and 1-octadecene (39.28 kJ/mol for n-decane and 54.27 kJ/mol for 1-octadecene) in addition to the difference in the standard boiling temperature because the former is closely related to the number of fuel molecules and oxygen available for chemical reaction after the fuel evaporation. The standard boiling temperature of 1-octadecene is about 140 K higher than that of n-decane and the molar latent heat of 1-octadecene is 40% greater than that of n-decane. This large latent heat and boiling temperature, which behave as large heat loss, lead to the low flame spread rate on the 1-octadecene droplet array because the unburned droplet is heated and ignited by the burning droplet, resulting in the flame spread phenomena.

It is interesting to see in Fig. 4 that, for the blended fuel, the flame spread rate is large in the lower pressure range and the pressure dependence is very close to that of n-decane. However, when the pressure increases further and exceeds the critical pressure of the blended fuel (2.56 MPa), the flame spread rate decreases quickly and becomes almost equal to that of 1-octadecene. The mechanism of the pressure dependence of the flame spread rate for the blended fuel will be discussed in the next section.

Flame Spread Mechanism of a Blended Fuel Droplet Array

To clarify the mechanism of the pressure dependence of the flame spread rate for the blended fuel, the evaporation characteristics of the blended fuel should be considered. In this study, the equilibrium conditions of the gas and liquid phases for binary fuel were calculated. As for the calculation, the Peng-Robinson state equation was employed at pressures below 1.13 MPa, and the equilibrium condition was determined so that the fugacity of the gas phase becomes equal to that of the liquid phase. When the Peng-Robinson state equation was used, the experimental values named Peng-Robinson parameters, which represent the inter-molecular force of mixture at high pressure, are needed. In this study, therefore, the Soave-Redich-Kwong state equation was used at pressures over 1.11 MPa. The accuracy of this state equation was not as good as that of the Peng-Robinson state equation, but no experimental parameters for a two-component mixture was needed. Comparison between the estimated values using these two equations proved that the differences in temperature and molar fraction at the equilibrium condition at 1.0 MPa were less than 1% and less than 3%, respectively. Therefore, depending on the pressure range, these two state equations were used in this study. Calculations of the equilibrium condition were conducted at pressures of 0.1 MPa, 0.5 MPa, 1.5 MPa, 2.0 MPa, and 2.3 MPa.

When pressure rises, the equilibrium conditions of both the liquid and gas phases shifted to a higher temperature. Around 1.5 MPa, the shifting of the gas phase curve to a higher temperature stopped and only the liquid curve shifted further, narrowing the range of the n-decane molar fraction in which the fuel is in subcritical condition. For example, at 1.5 MPa, the liquid-gas equilibrium state for fuel having an n-decane molar fraction of zero (i.e., a 1-octadecene mole fraction of 1.0) does not exist because the pressure at this state is

higher than the critical pressure of 1-octadecene. At 2.0 MPa, the curves of the gas phase and the liquid phase almost overlap. At 2.3 MPa, the liquid-gas equilibrium state does not exist for an n-decane molar fraction of 1.0 because the pressure is over the critical pressure of n-decane. At this pressure, however, the liquid-gas equilibrium state exists for the n-decane molar fraction of 0.62, which is the experimental condition of this study, because the critical pressure of the blended fuel is larger than that of both n-decane and 1-octadecene.

Figure 5 shows the vapor pressure curves of the two single-component fuels and the blended fuel. At each pressure, the boiling temperature is between those of n-decane and 1-octadecene, while the critical pressure is higher than those of the two single-component fuels.

For flame spread of a fuel droplet array, the fuel evaporates when the unburned droplet is heated by the flame of a burning droplet and the surface temperature reaches the level of the wet bulb temperature. The change in the vapor composition during the heating can be estimated from the temperature-composition relations at various pressures.

Figure 6 indicates the differences in the fuel vapor composition at 0.5 MPa and 2.3 MPa. In this figure, when temperature increases at of an n-decane molar fraction of 0.62, it reaches the liquid phase curve at both pressures. At 0.5 MPa, the equilibrium temperature is 560 K, corresponding to the boiling temperature at this pressure. The molar fraction of n-decane at the intersection point between the horizontal line of this equilibrium temperature and the gas phase curve corresponds to that of the n-decane molar fraction in the fuel vapor, which is 0.94 at this pressure. This means that when a blended fuel whose n-decane molar fraction is 0.62 is heated at 0.5 MPa, the boiling point becomes 50 K higher than that of n-decane and the n-decane molar fraction in the fuel vapor becomes 0.94.

Figure 7 shows the variations of the n-decane molar fraction of fuel vapor with pressure estimated using the above-mentioned method, indicating that the n-decane molar fraction in the fuel vapor decreases with a rise in pressure. On the other hand, the 1-octadecene molar fraction in the fuel vapor increases with pressure, reaching almost the same molar fraction as that of the liquid phase at pressures over 2.0 MPa.

Based on the above-mentioned pressure effects on the molar fractions of the fuel vapor, explanations of the mechanism of pressure dependence of the flame spread rate for the blended-fuel droplet array seen in Fig. 4 are possible. The pressure dependence of the flame spread rate is similar to that of n-decane at pressures up to about 2.5 MPa, although the flame spread rate is slightly smaller than that of n-decane. This is because, as shown in Fig. 5, the boiling temperature of the blended fuel is 50 K higher than that of n-decane and the ignition time is slightly longer. The velocity of the fuel-vapor jet is also expected to be smaller. When the pressure was increased further and exceeded 2.5 MPa, the flame spread rate decreased drastically and became almost equal to that of 1-octadecene. This is because the gas-phase molar fraction became almost equal to the liquid phase molar fraction and the effects of 1-octadecene on the ignition time became significant.

As already stated, OH emission images of the spreading flame of the blended fuel at pressures over the critical pressure often

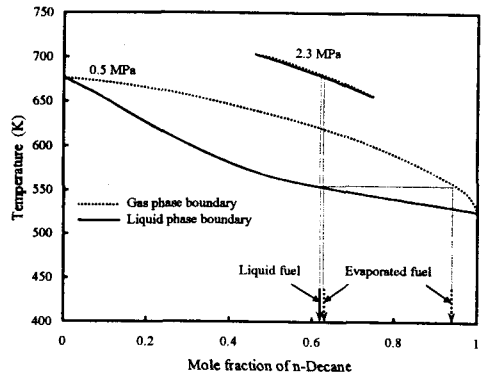

Fig. 6 Liquid-gas equilibrium curves of the blended fuel.

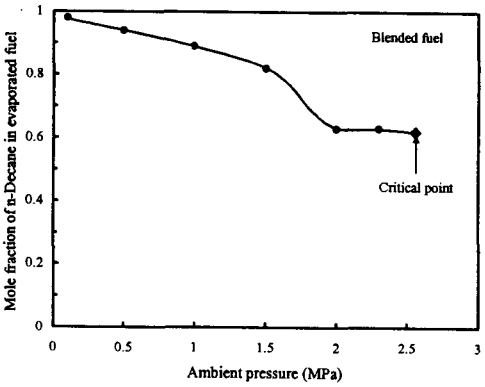

Fig. 7 Variations of n-decane molar fraction in the fuel vapor with pressure.

appeared to be zigzag and intermittent, indicating the occurrence of a fuel vapor jet. In this case, even though the fuel-vapor was ignited, the unburned droplet was not always ignited. It was observed from OH images that the ignition of the unburned droplet finally occurred after several fuel-vapor ignitions. This delay of the whole ignition is basically due to the characteristics of 1-octadecene. Therefore, we can say that at lower pressures, the flame spread characteristics of the blended fuel droplet array are predominated by n-decane because the most of the fuel vapor consists of n-decane. When the pressure rises and the molar fraction of 1-octadecene in the fuel vapor becomes close to the molar fraction of the liquid phase, the effects of 1-octadecene on the ignition time becomes significant and 1-octadecene becomes predominating for flame spread mechanism of the droplet array.

CONCLUSIONS

Flame spread experiments on a fuel droplet array for n-decane, 1-octadecene, and blends of the two (50%:50% vol.) were performed at pressures over the critical pressure in microgravity. High speed observations of the OH emission images of spreading flame were conducted and the flame spread rates were calculated based on the time history of the spreading forehead of the OH emission images.The following results were obtained:

1. The flame spread rate of 1-octadecene was found to be smaller than that of n-decane over the whole pressure range in this experiment.

2. The pressure dependence of the flame spread rate was highly affected by n-decane in the pressure range from atmospheric pressure to a pressure near the critical pressure of the blended fuel. When the pressure increased further, 1-octadecene became predominating for the flame spread mechanism.

3. These characteristics of the flame spread of the blended fuel were explained based on gas-liquid equilibrium states, that is, the fuel gas which evaporated from the droplet at ordinary pressure consists mostly of n-decane, whereas over the critical pressure, the composition of the fuel gas was almost the same as that of the liquid phase, resulting in a significant effect of 1-octadecene on ignition and flame spread at this higher pressure.

Acknowledgement

This research was supported by NASDA and the Japan Space Forum, under Ground Research Announcement for Space Utilization.

REFERENCES

1. Faeth, G. M., Dominicis, D. P., Tulpinsky, J. F., and Olson, D. R., *Proc. Combust. Inst.* 12: 9-18 (1969).
2. Yoshida, S., Hara, H., and Okajima, S., *JSME Trans.* Ser. B (in Japanese) 55: 1241-1247 (1989).
3. Kato, S., Kobayashi, H., Mizuno, H., and Niioka, T., *JSME Int. Journal. Ser. B*, 41: 322-330 (1998).
4. Park, J., Iwahashi, T., Kobayashi, H., and Niioka, T., *Fifth International Microgravity Combustion Workshop*, NASA, Cleveland, (1999), pp. 307-310.